DANMARKS OG GRØNLANDS GEOLOGISKE UNDERSØGELSE RAPPORT 2001/74

Diagenesis of the Silurian oil reservoir rock from the Kudirka Atoll in Lithuania

Niels Stentoft, Petras Lapinskas, Petras Musteikis
and Lars Kristensen

GEOLOGICAL SURVEY OF DENMARK AND GREENLAND
MINISTRY OF ENVIRONMENT AND ENERGY

GEUS

DANMARKS OG GRØNLANDS GEOLOGISKE UNDERSØGELSE RAPPORT 2001/74

Diagenesis of the Silurian oil reservoir rock from the Kudirka Atoll in Lithuania

Niels Stentoft, Petras Lapinskas, Petras Musteikis
and Lars Kristensen

GEOLOGICAL SURVEY OF DENMARK AND GREENLAND
MINISTRY OF ENVIRONMENT AND ENERGY

GEUS

The Upper Silurian limestone rocks of the Kudirka Atoll reef-complex show a complex diagenetic history. By thin section petrography on 50 samples from 7 wells the following sequence of diagenetic events (from oldest to youngest) could be established with a rather high degree of certainty: Compaction/dewatering → Early lithification → Insignificant fracturing → ?First generation of leaching → Precipitation of first generation of inter-/intra-granular calcite cement → Precipitation of second generation of inter-/intra- granular calcite cement → Recrystallization of lime mud, sparry calcite cements, and fossils → Chemical compaction with formation of stylolite-associated fractures → Precipitation of dolomite, pyrite and silica crystals → Second generation of leaching with stylolite surfaces acting as conduits for aggressive fluids → Oil emplacement. In all types of reef rock the late diagenetic leaching phase has favourably influenced the present reservoir quality (K and Φ). No clear correlation was found between rock texture and reservoir quality. The numerous crinoid fragments in samples of biosparite/biosparrudite and poorly washed biosparite/biosparudite are primarily responsible for that, as the rate of growth of syntaxial rimcement on the single-crystalline echinoderm fragments was far greater than the rate of growth of cement on associated multi-crystalline fossils. However, the calcite-replacing calcitic dolomite-crystals, that are associated with the stylolitic joints, have also in places contributed to the lacking correlation.

Authors' addresses

N.S & L.K., *Geological Survey of Denmark and Greenland,Thoravej 8, DK-2400, Copenhagen NV, Denmark.*

P.L., *Institute of Geology, T. Ševčenkos 13, 2600 Vilnius, Lithuania.*

P.M., *Vilnius University, Čiūrlionio 21/27, 2009 Vilnius, Lithuania.*

INTRODUCTION

In the Lithuanian part of the eastern borderland of the Baltic Syneclise the bulk of the known oil accumulations is found in Middle Cambrian sandstone reservoirs, but a great deal of oil shows have also been encountered in reefal carbonates and other limestones of both Ordovician and Silurian age (for reviews in English of the oil geology of the Baltic Syneclise see Brangulis *et al.*, 1992; Brangulis *et al.*,1993; Górecki *et al.*, 1992; Mokrik, 1998; Paškevičius, 1997; Ulmishek, 1990; and Zdanavičiūtė & Bøjesen-Koefoed, 1997). The idea that Silurian reef rocks from the Pridoli Stage are favourable for trapping of oil was proposed in 1964 by P. Lapinskas (cf. e.g. Lapinskas & Smilgis, 1972; and Lapinskas & Chechavichius, 1981), and during the prospecting for oil in 1983-1988 the Kudirka Atoll Field in the southern Lithuania was discovered and described by Lapinskas and other (cf. Lapinskas, 1987a, 1987b, 1993, 2000; and Lapinskas *et al.*, 1987). Their investigations showed that we are dealing with a large atoll-like reef structure of about 5×8 km, being up to 88 m in thickness (cf. Fig. 1), of which the upper part is occupied by oil accumulation. The oil field of Kudirka Atoll is thus related to lithologic traps with overlaying shaly carbonates acting as seals. The atoll itself shows a complex spatial distribution of the different reef facies, that is the fore-reef facies, the back-reef facies, the interior lagoonal facies, and the reef-crest facies, the latter being represented by stromatoporoid/crinoid build-ups. The oil is primarily found in the biosparitic and biolithic limestones of the reef-crest facies and the uppermost fore- and back-reef facies. However, an oil-production, in the proper sense, from the Kudirka Field has not yet taken place as the well-tests showed too low production rates, thus a pumping test from one of the most promising wells (Vilkaviškis 135, at a depth of 768-774 m) yielded only 3.38 m^3 heavy (0.8887 g/cm^3), gas-free oil per day (Paškevičius, 1997). The heterogeneity of the reservoir quality (porosity and permeability) of the reservoir rocks seems also to be influenced by a heterogeneous diagenetic alteration of the original sediments and reef rocks by leaching and cementation.

Our intention of the present paper is to provide an overview of the diagenetic phenomena in the reservoir rocks of the Kudirka Atoll, and to answer following questions: (1) Which diagenetic processes have occurred within the different reef rock types from the time of deposition until the present day? (2) Have the diagenetic events influenced the reservoir quality (Φ and K) of the different reef rocks in a different way?

Results from the study have previously been presented at two international conferences (cf. Stentoft *et al.*, 1998, 1999).

MATERIALS AND METHODS

The macroscopic and microscopic investigations, that form the basis of the description of the diagenetic history, are based on core material from following wells of the Kudirka Atoll field: Vilkaviškis-126, -131, -132, -135, -136, -137 and –139 (cf. Lapinskas *et al.*, 1987). A total of 50 thin sections (30 μm thick) were prepared from plug samples (cf. Fig. 2) and examined in transmitted light. Half of each section was stained with Alizarin Red S and potassium ferricyanide ($C_{14}H_7NaO_7S \cdot H_2O$ and $K_3(Fe(CN)_6)$ respectively) in order to facilitate the distinction between calcite and dolomite, and to delineate ferroan phases (cf. Dickson, 1966). Fourteen of the thin sections were examined under an incident-light fluorescence microscope with blue-light excitation filter to recognise depositional

textures, and to identify growth zones in calcite and/or dolomite cements. To see whether the carbonate crystals, that were assumed to be dolomite, are in fact pure, or close to pure $CaMg(CO_3)_2$, two thin sections were polished and examined by SEM-ED. Three polished and unstained thin sections were analysed for Fe, Mg, Sr and Mn with an electron microprobe (JEOL JCXA-733). A beam spot diameter of 20 μm was used with an accelerating potential of 15 kV and a specimen current of 50 nA. Count integration time was approximately 20 seconds. Siderite, magnesite, celestine and rhodochrosite were used as standards for Fe, Mg, Sr and Mn, respectively. A total of 15 plugs were picked out for capillary pressure measurements by means of the porous plate method, using distilled water as wetting phase and air as non-wetting phase. Small rock pieces from these plugs were examined by SEM. The classification of the rock sections follows Folk (1962) and Friedman (1965). In the description of cements the nomenclature of Bathurst (1976) is usually used. The crystal size scale is from Folk (1962):

ECxn	Extremely coarsely crystalline	> 4 mm
VCxn	Very coarsely crystalline	1-4 mm
Cxn	Coarsely crystalline	0.25-1 mm
Mxn	Medium crystalline	62-250 μm
Fxn	Finely crystalline	16-62 μm
VFxn	Very finely crystalline	4-16 μm
Axn	Aphanocrystalline	< 4 μm

RESULTS

Rock types and original sediments

The 50 thin sections that were used in the elucidation of the diagenetic history represent a 3 km long and 1 km wide rock body, being up to about 50 m thick. According to Folk (1962) these sections could texturally be classified as shown in Fig. 2. The corresponding original sediments are undoubtedly as follows, being arranged with increasing current intensity when they were deposited: Biomicrite and biomicrudite = skeletal lime mud. Poorly washed biosparite and biosparrudite = skeletal lime sand and skeletal lime sand/gravel respectively, with interstices being partly filled with lime mud. Biosparite and biosparrudite = skeletal lime sand and skeletal lime sand/gravel respectively. Biolithite = framebuilders that have grown, and remained in place, in a reef-crest facies (reef core), or biohermite, being pebble to cobble sized debris from framebuilders.

Cements

The reservoir quality of all the above-mentioned rock types has been unfavourably influenced by precipitation of sparry calcite cement, but also dolomite crystals, that are usually connected with pressure-dissolution structures, play an important part, by reducing porosity and permeability, in many of the samples.

Calcite cement

As for the intergranular calcite cement, the crinoid fragments have played a particular part. These fragments are, in fact, responsible for the greatest diagenetic change by rock volume of 2/3 of the samples, being biosparites/biosparrudites and poorly washed biosparites/biosparrudites (cf. Fig. 3). That is because the rate of growth of syntaxial rimcement on single-crystalline echinoderm fragments was far greater than the rate of growth of cement on associated multi-crystalline fossils, built up of tiny crystals. Growth zones are found in the crinoid rimcement crystals (cf. Fig. 4). Alizarin Red S stain and blue-light fluorescence usually reveal two zones, but three or more zones are locally seen in six of the fourteen samples examined by blue-light fluorescence. Sporadically, the zonation can also be seen faintly in the non-stained part of the sections because the innermost (the oldest) cement zone is a little more rich in tiny little inclusions. The rimcement, or at least the latest accretion of the crystals, seems not to have been precipitated quite "passively", as it has in places partly replaced multi-crystalline skeletal grains, and skeletal grains with associated earlier isopachous cement, being scalenohedral in habit. The presence of the growth zones is confirmed by the microprobe analyses. Certainly, the contents of magnesium and iron showed to be very small in all the calcites that were measured (contents of Sr and Mn could not be detected), but some difference was found between the oldest rim-cement (zone I), inside which the crinoid fragment appears as dusty inclusions, and the youngest one (zone II), cf. Fig. 5. No magnesium and iron at all could be detected in the latter zone.

The intergranular as well as the intragranular sparry cement connected with multi-crystalline fossils have also grown in a stepwise manner, as two generations of spar are usually seen: an earlier generation forming a fringe of scalenohedral crystals, and a later one being rhombohedral in habit (cf. Fig. 7 and Fig. 8a). The isopachous, scalenohedral calcite crystals have a ghost-like appearance because they recrystallized (neomorphism) contemporaneously with the recrystallization of the fossils themselves. The later blocky cement may be a former "passive" cement that recrystallized at the same time, because it shows fabric criteria for neomorphic spar, that is a xenotopic fabric and indistinct contacts between spar and surrounding calcite. The sparry calcite cements in former shelter pores and in a few, small fractures seem also to be a neomorphic spar (cf. Fig. 8b and Fig. 8a respectively).

In the samples of biomicrite and biomicrudite (cf. Fig. 2) irregular patches of spar are commonly seen. These irregular bodies of medium crystalline to very coarsely crystalline calcite spar are relatively most common in the biomicrite sample from well 137, this sample partly being a dismicrite (cf. Folk, 1959). The origin of these spar-filled openings (mudcracks?) is not known to the writers, however, the presence of geopetal sediment, a recrystallized lime ooze, beneath some of the sparry patches may indicate that the irregular openings were formed relatively early in the diagenetic history, either by an infaunal activety (by burrowing animals, cf. the faintly mottled appearance of the biomicritic rocks) or by leaching, before the sediment was lithified, when the substrate was composed of a stiff, but uncemented sediment, a "firmground" *sensu* Ekdale *et al.* (1984). The contact between patches and surrounding aphanocrystalline to very finely crystalline matrix is never sharp, and the spar itself shows a xenotopic, sutured mosaic fabric, which render it very likely that we are dealing with a neomorphic spar, perhaps a former "passive cement" that has been recrystallized. The curved (saddle-shaped) course of the content (in wt-%) of magnesium and iron along a microprobe traverse that crosses a patch of sparry cement seems to support those state of things (cf. Fig.6).

With high magnification of the microscope former lime mud is observed to consist of a sutured mosaic of aphanocrystalline to very finely crystalline calcite crystals. (Fig. 9) The mud has surely been

altered by neomorphism. The multi-crystalline fossils have also been more or less replaced by micrite and/or microspar (cf. Fig. 10), they are in places so micritized that they can be classified as peloids (cf. Fig. 3).

Dolomite cement

The degree of dolomitization in volume % of the 50 thin sections is shown in Table 1. The four samples in which the dolomite play an important part by reducing the porosity and the permeability of the rocks are as follows:

- A biosparrudite from well no. 126 (sample 126/3B) with $^1/_3$ – $^1/_2$ of the rock volume being occupied by dolomite.
- A biosparite from well no. 131 (sample 131/4B) with about 20 % of the rock volume being dolomitized.
- A biosparite from well no. 136 (sample 136/5B) with $^1/_2$ – $^3/_4$ of the rock volume being dolomitized, and
- A poorly washed biosparrudite from well 136 (sample 136/6B) with about 50 % of rock volume occupied by dolomite.

In 7 of the samples no dolomite crystals were observed at all. Of the remaining 39 samples less than 2 % dolomite was observed in the 25, and 2 – 10 % in the last 14.

In thin section, under the petrographic microscope, the dolomitization is observed to be fabric selective, the precipitation of dolomite crystals being primarily connected with the pressure-dissolution structures (see below). However, rather few, scattered rhombohedral dolomite crystals are also precipitated in the aphanocrystalline to very finely crystalline matrix of 6 of the samples (biomicrite, biomicrudite and poorly washed biosparrudite).

The dolomite crystals themselves, that vary in size from very finely crystalline to coarsely crystalline, appear both as scattered rhombohedral crystals (cf. Fig. 11) and as crystal aggregates that usually show a hypidiotopic mosaic fabric (cf. Fig. 12). Finely-sutured contacts have not been observed between the dolomite crystals in these aggregates, and none of the crystals seems to have been subjected to neomorphic alteration like the surrounding fossils that have been more or less replaced by micrite and/or microspar. The only diagenetic event that has affected the dolomite is a dissolution: a late-diagenetic leaching that took place along the stylolitic joints (see below) has also in many places "attacked" dolomite crystals precipitated in the stylolites during or after the chemical compaction (cf. Fig. 13).

During their growth the dolomite crystals have indiscriminately replaced the carbonate around the stylolitic joints, both calcite cements, multi-crystalline fossils and single-crystalline crinoid ossicles. However, small, almost dusty, inclusions of calcite are seen in many of the dolomite crystals as if they have not always completely replaced the surrounding carbonate. In contrast to the above-mentioned sparry calcite cement no growth zones are revealed in the dolomite crystals by the Alizarin Red S stain or by the blue-light fluorescense.

The results of the SEM-ED analyses are shown in Table 2. The Ca/Mg atomic ratio vary from 1.2 to 1.4 with a mean of 1.3, and the Ca/(Mg + Fe) atomic ratio from 1.2 to 1.3 with a mean of 1.2, the latter ratio is on the assumption that Fe has substituted for Mg in the mineral. Note that small, but significant amounts of Fe is present in all the samples (1.2 – 2.1 atomic %, and 2.7 - 4.8 weight %).

Based on the Ca/Mg weight ratio the mineral may be classified as a *calcitic dolomite* according to Chilingar (1957), the Ca/Mg weight ratio being from 2.0 to 2.3 with a mean of 2.2. The Ca/(Mg + Fe) weight ratio is from 1.7 to 2.0 with a mean of 1.9. It is thus obvious that the dolomite crystals are not of an ideal stoichoimetric composition, given by the formula $CaMg(CO_3)_2$, and with the cation layers in the crystal composed alternately of pure Ca^{++} and pure Mg^{++}. Based alone on these few analyses the composition of the replacing dolomite mineral of the Kudirka Field is approximately as follows:

$$Ca_{1.10}Mg_{0.83}Fe_{0.06}(CO_3)_2$$

Porosity development

A rather late diagenetic leaching has favourably influenced the present reservoir quality (Φ and K) of all the rock types. After an event of chemical compaction aggressive fluids seem to have percolated the reef rocks via the insoluble residue accumulations of the pressure-solution structures. During the phase of chemical compaction distinct fitted fabrics with grain contacts being made of microstylolites were formed in all types of rock except for the biomicrites and biomicrudites (cf. Fig. 3 and 11). Rather few solution seams and "true" stylolites, usually poorly developed, were also formed during this phase, as were a few small tension gashes connected to stylolites in samples of biosparrudites and biolithites. In all the investigated samples a positive correlation is observed to exist between the amount of insoluble residuals and the extent of dissolution of surrounding calcite: the more insoluble matter present the more volumes of aggressive fluids have seemingly been able to attack surrounding rock. Numerous tiny solution vugs were formed along the pressure-solution structures (cf. Fig. 11 and 8b), and a widening of pre-existing intra/inter granular pores took place. The few tension gashes were solution-enlarged simultaneously. The rhombohedral dolomite crystals, that were precipitated contemporaneous with or after the chemical compaction, seem to have been corroded during the same event of leaching (cf. Fig. 13).

DISCUSSION

The diagenetic events arranged in relative time

All mineral phases or events assumed to be of importance for the present reservoir quality of the rocks were evaluated for relative timing of their genesis. Even some of the observed diagenetic events could not easily be arranged in relative time in all the investigated samples the following "flow-chart" for diagenetic evolution seems to apply for all the Kudirka reef rock types: (1) Original sediment → (2) Compaction/dewatering of lime mud → (3) Early lithification → (4) Formation of (a few) small fractures → (5) First phase of leaching → (6a) First step of precipitation of intergranular/intragranular sparry calcite cement → (6b) Second step of precipitation of intergranular/intragranular sparry calcite cement → (7) Recrystallization, a neomorphic alteration → (8) Chemical compaction and fracturing → (9) Precipitation of dolomite, pyrite and silica → (10) Second phase of leaching → (11) Oil emplacement → (12) Present rock.

As regards the early phase of leaching (phase 5), some irregular openings in former lime mud, that now appear as irregular patches of calcite spar of dismicritic texture, and a few small fractures (cf. Fig. 8a) appeared to be solution-enlarged before they became occupied by calcite cement.

Concerning the relative timing of the recrystallization (phase 7) some uncertainties are also present. The precipitation of the latest generation (growth zone) of the non-fluorescent, non-passive rimcement on crinoid fragments may thus have taken place in the same period of time. However, it is not at all unlikely that the recrystallization of the reef rocks have taken place stepwise during a large space of time; a renewed aggrading neomorphism of microcrystalline calcite is thus observed in some places, and recrystallization of fossils seems in places to have taken place either before or after the recrystallization of surrounding fine-grained matrix. Finally, one cannot exclude the possibility that the micritization of fossils was initiated even before the first generation of "passive" cement spar was precipitated (cf. Phase 6).

The relative timing of the precipitation of the three calcite-replacing crystals of phase 9 could not be established for certain. All three may have been nucleated contemporaneously with the chemical compaction.

The calcite-replacing dolomite

The relationship between dolomitization and rock texture

Assuming that the results of the SEM-ED analyses (Table 2) carried out on only two samples from two of the wells are representative of the dolomite all over the Kudirka reef structure we would be able to state:

1. That the spatial variation in the reef structure of the content in atomic % of the elements Ca, Mg and Fe is small, and
2. That no noticeable variation of the element ratios seems to exist inside one and the same dolomite crystal, that means no crystal-zonation is found like in the calcite rimcement crystals.

Some indications thus seem to show that the precipitation of the dolomite (phase 9), which took place contemporaneous with or after the chemical compaction (phase 8), represents one single event being accomplished during a geological short period of time. However, no trend of the spatial distribution of the dolomite seems to exist: no increase in the content of dolomite is seen downwards in the reef structure, and no dolomitization "front" is seen neither from west to east (well 131, 126 and 135, cf. Fig. 1) nor from north to south (well 137, 139, 132, 135 and 136, cf. Fig. 1). This may simply be due to the fact that a total of 50 rock samples is too scanty to elucidate the conditions in such a big and complex reef structure. Another cause of the apparently random degree of dolomitization may be due to the fact that the appearance of the Mg^{++}-rich fluids within the reef rocks was selective being determined by the local sizes of the chemical compaction. It appears from Table 1 that there is a correlation between volume % dolomite and rock texture as most dolomite has been precipitated in biosparites and biosparrudites, whereas relatively very little, or nothing at all, dolomite has been precipitated in biomicrites and biomicrudites. Exactly the sparitic rocks are very rich in stylolitic grain contacts as they usually show a more or less well-developed fitted fabric (containing interpetrant particles, primarily consisting of poorly preserved crinoid fragments embedded in their calcite rimcement, cf. Fig 3, but "true" stylolites (cf. Fig. 11) are also seen. In the micritic rocks, on the other hand, the dolomite crystals are only connected to few stylolites and/or appear as a few scattered

rhombohedrals in the micrite matrix. The dolomite in the biolithic rocks (cf. Table 1) is also connected to the presence of pressure-dissolution structures: either the stylolitic grain contacts in former infiltered crinoid sand, that was transformed into biosparite with fitted fabric during the diagenesis, or stylolites developed in the contacts between coral or stromatoporoid colonies and biosparite, and in the contacts between two successive growth layers in a composite stromatoporoid colony.

The possible reason for the dolomitization

Because of its close connection to stylolites the dolomite was probably precipitated during a time when the reef sediments were buried to an adequate depth of minimum for the outset of the chemical compaction of the calcite. This means that the mixed-water or dilution model for dolomitization can be ruled out (cf. Morrow, 1982). If the chemical compaction took place in depths, let us say between 400 and 600 metres the dolomitization temperature may only have been from 33° to 40°C, assuming a geothermal gradient of 1°C/30 m and a sea bottom temperature of 20°C around the original crinoid-coral-stromatoporoid reefs. The studied rocks show no signs of unusual temperature/pressure conditions for the dolomitizations. No tectonic stylolites, slickensides or other structures are seen that may indicate that deformational forces other than those involved in simple burial prevailed.

Similar calcite-replacing burial dolomite cements being in some way associated with stylolites have been described from a series of carbonates representing several periods of the geological record, e.g. Mattes & Mountjoy, 1980 (Devonian); Lee & Friedman, 1987 (Ordovician); Zenger & Dunham, 1988 (Silurian/Devonian); and Moss & Tucker, 1995 (Cretaceous). One of the following two models, or a combination of both, is usually used to explain the cause of dolomitization in the buried calcite rocks: (1) the Burial Compaction Model where the Mg^{++}-bearing fluids, that move through the rock, are expelled from compacted shaly sediments (cf. Morrow, 1982), or (2) the Pressure Solution Model, after which the Mg^{++} are supposed to originate from the calcite crystals that are dissolved during the formation of the stylolitic joints, that is a "solution cannibalization" (cf. Wanless, 1979). That is true that Zenger & Dunham (1988) are not giving preference to any particular dolomitization model in their description of a "stylolite-controlled" replacive dolomite, but Lee & Friedman (1987) as well as Mattes & Mountjoy (1980) incline to the opinion that the Pressure Solution Model has worked, and Moss & Tucker (1995) assume that the Mg^{++} necessary for dolomitization were carried to the platform carbonates via connate fluids from compaction of basinal mud below the platform in accordance with the Burial Compaction Model.

The low content of magnesium in the calcite of the Kudirka reef rocks (cf. Fig. 5 and Fig. 6), which to some extent is in accordance with the usual early diagenetic (pre-burial) conversion of high-magnesian calcite to low-magnesian calcite, seems immediately to speak in favour of the Burial Compaction Model as an explanation of the dolomitization. If we assume that that is the fact the stylolite-associated dolomite crystals may here have been precipitated because Mg^{++} were expelled from the underlaying or laterally situated marine clay deposits. The stylolitic joints in the reef rocks may then have acted as conduits for the Mg^{++}-bearing fluids. If so, the Ca^{++} being set free during the chemical compaction should have reacted with Mg^{++} in a liquid mixture that under the conditions in question was subsaturated with respect to calcite but supersaturated with respect to dolomite, or at least a calcitic dolomite. However, two circumstances suggest that pressure dissolution (the Pressure Solution Model) has caused the dolomite precipitation, at least locally in the Kudirka reef system: Firstly, dolomite crystals are observed to overlie poorly developed stylolites and solution seams formed

in small isolated areas where a percolation of fluids from outside must have been extremely limited at the time when the chemical compaction took place, for instance inside stromatoporoid colonies that show a massive sutured mosaic fabric because they have previously been neomorphic altered (cf. Fig. 14). For that reason it is obvious to assume that the Mg^{++} essential to the dolomitization stem from the surrounding calcitic rock being dissolved during the chemical compaction. Secondly, the 5 samples of crinoid biosparite and biosparrudite from well nr. 139 (cf. Fig. 1) seem to make the Burial Compaction Model unlikely. The present relatively high porosity and permeability of these rocks are to a high degree connected to the solution-enlarged, inter-granular micro-stylolites (in areas of fitted fabric), but a great part of the inter-granular spaces are here assumed to be original interstices that have never been completely occupied by crinoidal rimcement during the diagenetic history. Even the rimcement around the crinoid fragments has suffered some damage because of a late-diagenetic corrosion (phase 10) the original rhombohedral crystal-faces appear still almost intact, as in any calcite cement lining a cavity which it fills incompletely. The rocks from well 139 may thus have been fairly permeable and porous when the assumed Mg^{++}-bearing fluids were introduced, and they might have been percolated by relatively many pore-volumes of these fluids. However, very little dolomite was nevertheless precipitated, less than 1 volume-% actually, and the dolomite rhombohedrals are preferably precipitated in the micro-stylolitic grain contacts in areas showing a fitted fabric, not in the inter-granular pores being incompletely filled in with calcite rimcement, as if the dolomitization took place according to the Pressure Solution Model. In spite of the presumably small content of Mg in surrounding calcite, both the fairly low Mg/Ca values in the dolomite crystals (Table 2) and the rather low degree of dolomitization in the reef rocks in general (Table 1) may speak in favour of the last mentioned model.

The environment for the second phase of leaching

Both the fact that the porosity created during the second phase of leaching (phase 10) is closely associated to the stylolitic joints, and the general burial history of the Kudirka reef sediments (see below), make it likely that this leaching took place under deep-phreatic conditions. An uplift of the reef rocks to the vadose zone (in a subaerial meteoric environment) from a depth of burial where stylolites could be formed (phase 8) can hardly have taken place.

During the last two decades it has been demonstrated by several geologists that a dissolution can, in fact, take place after the carbonate sediment is buried to depths of many hundreds of metres, and that such mesogenetic dissolutions may play a considerable part for the improvement of the reservoir quality (Φ and K), cf. e.g. Mazzullo & Harris (1992) who list no less than 27 examples from the literature of mesogenetic dissolution of limestones and dolomites. The phenomenon is not quite unknown either to the writer (NS), who has observed it from both Late Devonian carbonates of the Vetkhin and Devonian Fields in Belarus, Zechstein carbonates from South Jylland in Denmark, Upper Jurassic limestones from the Abadia Structure in Portugal, and Upper Cretaceous chalks of the Dan Field in the Danish North Sea (Stentoft, 1990; and unpublished reports).

It is probably most likely that the aggressive fluids, that cause the deep-burial dissolution of calcite and dolomite, evolve by addition to pore fluids of CO_2, organic acids and/or H_2S generated from the organic-matter maturation prior to the release of the hydrocarbons from the source rocks, or during the later hydrocarbon degradation, cf. the discussion on the potential sources for aggressive fluids in Mazzullo & Harris (1992). In the Kudirka field the aggressive fluids may have migrated from the underlaying and/or laterally situated shaly source sediments (probably Silurian, cf. Zdanavičiutė &

Bøjesen-Koefoed, 1997) because of the burial compaction, and subsequently entered the carbonate reef rocks via the stylolitic joints that at the same time got more or less solution-enlarged. The formation of such a deep-burial secondary porosity, being associated with and along stylolites, has also been described by several authors during the last two decades (e.g. Mazzullo, 1981; Dravis, 1989).

Possible relationship between diagenetic events and burial history

It is quite obvious to try to relate some of the diagenetic phases to the burial history revealed by the curve of burial for a Kudirka well shown in Fig. 15. This well (Kudirka-145) is situated about 850 m NNE of well 131 (cf. Fig. 1). The phase of chemical compaction (cf. phase 8 above) is thus assumed to have taken place during the rapid burial in Triassic time when the Kudirka reef rocks got buried to the adequate depth of minimum for formation of stylolites. The later leaching (cf. phase 10 above), which post-dates the chemical compaction, may be related to the subsequent tectonic phase of uplift in Early Jurassic. The dolomite (phase 9 above) is as we have seen introduced before this late phase of leaching, but after or contemporaneous with the chemical compaction.

The first five diagenetic events (phase 2-6a above) are supposed to have taken place in late Silurian, in a very shallow burial, or syngenetic, stage, whereas the precipitation of the second generation of calcite cement (phase 6b) is supposed to have taken place in a shallow burial or epigenetic stage, perhaps in Early Devonian time.

Relationships between rock texture and reservoir qualities

Ancient reef structures are generally assumed to be of great economic significance because they are good traps for oil and show rather high porosities (cf. e.g. Toomey, 1981, and Rieke *et al.*, 1996). The oil production from reef reservoirs comes from the biolithic reef-crest facies and/or the proximal slope facies, whereas lagoonal facies usually are very poor reservoirs. However, in the present reef rocks of Kudirka primary porosity of some importance is for some reason only preserved in the proximal fore-reef biosparitic and biosparruditic rocks from one of the investigated wells (well V-139, cf. above). Otherwise no clear relationships between rock fabric and porosity could be seen during the examination of the rock samples (cores, plugs and thin sections). In the potentially good reservoir rocks, originally deposited in the proximal fore-reef facies, the ubiquitous rimcements on single-crystalline crinoid fragments, in places together with stylolite-associated dolomite crystals, have effectively blocked up the former interstices, and neither the early nor the late diagenetic leaching have been strong enough to create a good reservoir rock in any of the rock types. The many small solution vugs formed during the late phase of leaching are generally very poorly interconnected. Besides that, practically no natural fracturing has enhanced the reservoir quality in any of the investigated samples (cf. phase 4 and 8 of the diagenetic history).

To see if any correlation altogether could be demonstrated between texture (biomicrite, biosparite etc.) and reservoir quality, the textures determined by study of thin sections and core pieces used for plugging were plotted as a function of porosity and permeability respectively, the latter being based on the measurements on the corresponding plugs cf. Fig. 16 and 17. The expected pattern of texture versus reservoir quality, with biomicrites of lagoonal facies and biolithites of reef-core facies showing poor

qualities compared to both biosparites and biosparrudites of proximal foor-reef facies, is not manifested in the cross-plots. On the contrary, the biomicrites generally showed a better reservoir quality than the poorly washed biosparites and biosparrudites, and their quality differed only insignificantly from that of the biosparites and biosparrudites.

Capillary pressure data, deduced from capillary pressure curves, are very important when the reservoir quality of a rock is estimated. Good reservoir rocks show thus (1) low entry pressure, i.e. the pressure at which the non-wetting phase (here air) is present in the pore system as a continuous phase, (2) low irreducible water saturation (Swir in %), and (3) a fine sorting of the pore-throat size, where the sorting is a measure of degree of spread from the finest to the largest pore-throats. None of the 15 samples depicted for capillary pressure measurements gave a well defined irreducible water saturation, and only 5 of the samples, all being biosparites or biosparrudites, proved to be of fair reservoir quality, having a good producing potential, cf. Table 3.

The very high Swir-values of 32-97 % at 160 psi of the remaining 10 samples, representing both biomicrite, poorly washed biosparite/biosparrudite, biosparite, biosparrudite, and biolithite, seem to confirm the impression the writers had received during the examination of the thin sections: the many small solution vugs being generally very poorly interconnected. These rocks show a very poor, or nothing whatsoever, producing potential.

CONCLUSION

(1) The Kudirka reef rocks have been subjected to a complex diagenetic history. A total of at least 11 diagenetic phases has thus been recorded, but the present porosity and permeability (the reservoir quality) of the rocks is primarily linked to two or more phases of inter-/intra-granular cement precipitation and a phase of late diagenetic leaching. However, the precipitation of stylolite-associated dolomites crystals also play an important part in several places.

(2) Irrespective of the site in the investigated part of the Kudirka reef complex, and irrespective of the rock type (the rock texture), the reef carbonates have all been subjected to the same sequence of diagenetic events.

(3) The diagenetic transformation of the Kudirka reef rocks has ruined the expected relationships between reservoir quality and reef facies (rock texture): the proximal fore-reef facies (biosparite/biosparrudite) being of good quality and the lagoonal facies (biomicrite/biomicrudite) of relatively very poor quality.

REFERENCES

Bathurst, R.G.C., 1976, Carbonate sediments and their diagenesis. *Development in Sedimentology,* v. 12, Elseviers Scientific Publishing Company, Amsterdam, 658 pp.

Brangulis, A.P., Kanev, S.V., Margulis, L.S. & Haselton, T.M., 1992, Hydrocarbon geology of the Baltic Republics and the adjacent Baltic Sea. *In*: H.A.M. Spencer (ed.), Generation, accumulation and production of Europe's hydrocarbons. Special Publication of the European Association of Petroleum Geoscientists No. 2, p. 111-115.

Brangulis, A.P., Kanev, S.V., Margulis, L.S. & Pomeranseva, R.A., 1993, Geology and hydrocarbon prospects of the Paleozoic in the Baltic region. *In*: J.R. Parker (ed.), Petroleum Geology of Northwest Europe: Proceedings of the 4th Conference (vol. 1), Geol. Soc. Lond., p. 651-656.

Chilingar, G.V., 1957, Classification of limestones and dolomites on the basis of Ca/Mg ratio. *J. Sedim. Petrol.*, v. 27, p. 187-189.

Dickson, J.A.D., 1966, Carbonate identification and genesis as revealed by staining. *Jour. Sed. Petrology*, v. 36, p. 491-505.

Dravis, J.J., 1989, Deep-burial microporosity in Upper Jurassic Haynesville oolitic grainstones, East Texas. *Sedimentary Geology*, v. 63, p. 325-341.

Ekdale, A.A., Bromley, R.G. & Pemberton, S.G., 1984, Ichnology. The use of Trace Fossils in Sedimentology and Stratigraphy. *Soc. Econ. Paleontologists Mineralogists,* Tulsa, Okl., 317 pp.

Folk, R.L., 1959, Practical petrographic classification of limestones. *Bull. Am. Assoc. Petrol. Geologists*, v. 43, p. 1-38.

Folk, R.L., 1962, Spectral subdivision of limestone types. *In*: W.E. Ham (ed.), Classification of Carbonate Rocks. Am. Assoc. Petrol. Geologists, Tulsa, Okla., p. 62-84.

Górecki, W., Lapinskas, P., Lashkova, L., Lashkov, E., Reicher, B., Sakalaukas, K. & Strzetelski, W., 1992, Petroleum perspectives of the Baltic Syneclise. *Pol. J. of Min. Res.* 1, p. 65-88.

Lapinskas, P.P., 1987a, Silurian formations of Baltic Depression. *In*: R.G. Goretskyj & P. Suveizdis (eds.), Tektonika, fatsii i formatsii zapada Vostochno – Evropeiskoi platformy. Minsk: Nauka i Technika, p.103-116. (Translated from Russian)

Lapinskas, P.P., 1987b, Silurian system. *In*: G. Vosylius (ed.), Oil deposits of the Baltic area. Vilnius: Mokslas Publishers, p. 35-46. (Translated from Russian)

Lapinskas, P.P., 1993, Investigations of the Silurian Lithology in Lithuania and its practical significance. *Geologijos Akirãciai*, nr. 4 (12), p. 23-28. (In Lithuanian with English abstract).

Lapinskas, P.P., 2000, Structure & Petroliferosity of the Silurian in Lithuania. Institute of Geology, Vilnius, 203 pp.

Lapinskas, P.P., Malinauskas, J., Vaiceliunas, J. & Jacyna, J., 1987, New data on the geological structure of the Kudirka oil-bearing reef. *Geologija*, v. 8, p. 72-76. (Translated from Lithuanian).

Lee, Y.I. & Friedman, G.M., 1987, Deep-burial dolomitization in the Ordovician Ellenburger Group carbonates, West Texas and Southeastern New Mexico. *Journal Sed. Petrol.*, v. 57, p. 544-557.

Mattes, B.W. & Mountjoy, E.W., 1980, Burial dolomitization of the Upper Devonian Miette buildup, Jasper National Park, Alberta. *S.E.P.M., Special Publication*, No. 28, p. 259-297.

Mazzullo, S.J., 1981, Facies and burial diagenesis of a carbonate reservoir: Chapman Deep (Atoka) field, Delaware basin, Texas. *AAPG Bulletin*, v. 65, p. 850-865.

Mazzullo, S.J. & Harris, P.M., 1992, Mesogenetic Dissolution: Its role in Porosity Development in Carbonate Reservoirs. *AAPG Bulletin*, v. 76, p. 607-620.

Mokrik, R., 1998, Origin of the Baltic oil. *Geologija*, nr. 23, p. 25-30.

Moore, C.H., 1989, Carbonate diagenesis and porosity. *Development in Sedimentology*, v. 46. Elsevier, Oxford, 338 pp.

Morrow, D.W., 1982, Diagenesis 2. Dolomite – Part 2. Dolomitization Models and Ancient Dolostones. *Geoscience Canada*, v. 9, p. 95-107.

Moss, S. & Tucker, M.E., 1995, Diagenesis of Barremian-Aptian platform carbonates (the Urgonian Limestone Formation of SE France): near-surface and shallow-burial diagenesis. *Sedimentology*, v. 42, p. 853-874.

Musteikis, P. & Juškutė, V., 1999, Late Silurian brachiopod communities from western Lithuania. *Geologija*, nr. 27, p. 10-25.

Paškevičius, J., 1997, The Geology of the Baltic Republics. Vilnius University & Geological Survey of Lithuania, Vilnius, 387 pp.

Rieke, H.H., Chilingarian, G.V. & Mazzullo, S.J., 1996, Performance and classification of Carbonate reservoirs. *In*: G.V. Chilingarian, S.J. Mazzullo & H.H. Rieke (eds.), Carbonate Reservoir Characterization: A Geologic-Engineering Analysis, Part II. Devel. In Pet. Science, v. 44, Elsevier, p. 231-547.

Stentoft, N., 1990, Diagenesis of the Zechstein Ca-2 carbonate from the Løgumkloster-1 well, Denmark. *Geological Survey of Denmark*, Series B, No. 12, 42 pp.

Stentoft, N., Lapinskas, P.P. & Musteikis, P., 1998, Diagenesis of the Silurian reservoir rock from the Kudirka Atoll in Lithuania. *In*: Suveizdis, P. & Zdanavičiūtė, O. (eds), Perspectives of petroleum exploration in the Baltic Region. Proceedings of the Internal Conference 21-24 October 1998, Vilnius, Lithuania, p. 36-42.

Stentoft, N., Lapinskas, P.P. & Musteikis, P., 1999, Diagenesis of the Silurian reservoir rocks from the Kudirka Atoll, Lithuania. (Abstract). 19th Regional European Meeting of Sedimentology, IAS, Copenhagen, p.243.

Toomey, D.F., 1981, European Fossil Reef Models. *S.E.P.M., Special Publication*, v. 30, 546 pp.

Ulmishek, G., 1990, Geologic evolution and petroleum resources of the Baltic Basin. *In*: M.W. Leighton et al. (eds.), Interior Cratonic Basins, AAPG Memoir 51, p. 603-632.

Wanless, H.R., 1979, Limestone response to stress: pressure solution and dolomitization. *Journal Sed. Petrol.*, v. 49, p. 0437-0462.

Zdanavičiūtė, O. & Bøjesen-Koefoed, J.A., 1997, Geochemistry of Lithuanian oils and source rocks: a preliminary assessment. *J. Pet. Geol.*, v. 20(4), p. 381-402.

Zenger, D.H. & Dunham, J.B., 1988, Dolomitization of Siluro-Devonian limestones in a deep core (5,350 m), Southeastern New Mexico. *S.E.P.M.*, No. 43, p. 161-173.

FIGURE AND TABLE CAPTIONS

Fig. 1. Location map and the Kudirka Atoll structure (modified from Musteikis and Juškutė (1999), and Lapinskas (2000)). 1) argillaceous limestone; 2) marlstone; 3) clay/claystone; 4) micritic limestone; 5) biosparitic, biosparuditic and biolithic limestone; 6) eastern limit of the atoll according to the well data; 7) limit of the central atoll part according to the seismic data; 8) isohypses of atoll top; 9) location of the Vilkaviškis wells from where core samples have been picked up and used in the present study (cf. Fig. 2).

Fig. 2. The distribution in depth of the 50 rock samples used in the description of the diagenetic history, together with a specification of their texture (cf. Folk, 1962). The dotted line marks the approximate position of top reef-structure defined by the gamma ray log responses.

Fig. 3. Thin section photomicrograph (plane polarized light) of a biosparite. The rock has a fitted fabric, as most of the contacts between the syntaxial calcite cements, that surround the poorly preserved crinoids, consist of microstylolites. Besides the crinoid fragments a few peloids and a brachiopod fragment (B) are also seen. Scale of bar equals 300 μm.

Fig. 4. Thin section microphotographs showing growth-zones in syntaxial cement. With the use of plane polarized light (figure a) two growth-zones are dimly seen (I and II). Two growth-zones are distinctly illuminated with use of blue-light fluorescence (figure b): a brightly fluorescent earlier generation, forming a thin "border" around the crinoids, and a non-fluorescent later generation occupying most of the intergranular spaces. Note that it is not exactly the same two growth-zones that are illuminated in the two photographs. Scale of bars equal 300 μm.

Fig. 5. Shows the content of magnesium and iron along an about 350 μ long microprobe traverse on a polished and unstained thin section of a crinoid biosparite. The detection limit is roughly indicated by the dashed line.

Fig. 6. The content of magnesium and iron along an about 1.2 mm long microprobe traverse that crosses a sparry patch of a dismicrite-like biomicrite. The dashed line roughly indicates the detection limit.

Fig. 7. Thin section photomicrographs of tabulate coral. Both corallite wall and tabula look blurred in plane polarized light (a) due to micritization. An isopachous cement, scalenohedral in habit, is dimly seen. The contacts between this cement and the coarse intraskeletal, xenotopic spar are not sharp. With fluorescence microscopy (b) it seems possible to delineate more clearly the distribution of the brightly fluorescent skeleton with (earlier) isopachous calcite and non-fluorescent (burial) equant calcite. Scale of bars equal 100 μm.

Fig. 8. Thin section photomicrographs (plane polarized light) of neomorphic spar. (a) Tabulate coral cut through by a fracture. The latter is partly obliterated by neomorphic, xenotopic, intraskeletal spar. The neomorphosis seems also to have affected the skeletal structure. (b) An area between sparfilled

shelter pore and crinoid biosparite. A dissolution seam is developed here during a phase of pressure solution. The peculiar, dusty streaks in the sparry mosaic is probably a former geopetal mud, that now appears as ghosts in the replacing, neomorphic spar crystals. Scale of bars equal 300 μm.

Fig. 9. The SEM-image shows the sutured mosaic fabric of the micritic matrix of a biomicrudite.

Fig. 10. Thin section photomicrograph (plane polarized light) of biomicrite. The figure shows an ostracod with geopetal sediment overlaid by sparry calcite cement. Both the geopetal mud and most of the shell wall have been neomorphic altered, being replaced by an aphanocrystalline to very finely crystalline calcite. Scale of bar equals 50 μm.

Fig. 11. Thin section photomicrograph (plane polarized light) of stylolitic grain contacts between crinoids, embedded in syntaxial spar, and part of a recrystallized stromatoporoid colony. Small rhombohedral dolomite crystals are precipitated in the seams. One of them is observed to overlie a seam (arrow). Some of the solution vugs, that postdate the pressure-solution, are not filled with blue-dyed resin. Scale of bar equals 300 μm.

Fig. 12. Dolomite (being the blue-green stained part) has partly replaced a coarse-grained calcite rock, consisting of crinoids embedded in syntaxial calcite cement. The crinoid fragments are diffuse and appear as dusty inclusions in the cement. The dolomite has a hypidiotopic fabric. Plane polarized light. Scale bar equals 300 μm.

Fig. 13. SEM-image showing a dolomite crystal that has been very corroded.

Fig. 14. Thin-section microphotograph (plane polarized light) of part of stromatoporoid colony with two dissolution structures (the relatively dark-coloured, Axn-VFxn calcite strings), that are assumed to be incipient solution seams. Sub- to euhedral dolomite crystals are observed to overlie the structures. Scale of bar equals 300 μm.

Fig. 15. The burial history of the Silurian Kudirka Atoll sediments.

Fig. 16. Cross-plot of rock texture versus porosity. Texture and porosity were found on the 50 plug samples (cf. Fig. 2).

A = biomicrites and biomicrudites; n = 6.
B = poorly washed biosparites and biosparrudites; n = 8.
C1 = biosparites (except for those from well V-139); n = 11.
C2 = biosparites (from well V-139); n = 4.
D = biosparrudites; n = 10 (+ 1 from well V-139).
E = biolithites; n = 9 (+ 1 from well V-139).
■ = mean of the n observations (from all wells except for V-139).
● = mean of the n observations from well V-139.
I = standard deviation.

Fig. 17. Cross-plot of rock texture versus permeability. The permeability was measured on the same 50 plug samples, that were used for porosity measurements. For further explanation see Fig. 16.

Table 1. Dolomitization (d) in volume-% of the 50 thin sections being arranged in accordance with their texture (cf. Fig. 2).

Table 2. The content of Ca, Mg and Fe in dolomite crystals. The SEM-ED measurements have been made on two crystals in each rock sample.

Table 3. The only samples among a total of 15 that show fair reservoir qualities, even their irreducible water saturation (Swir) at 160 psi are rather high. An air-pressure of 160 psi was the highest pressure step used in the pressure pots (in the porous plate method) for construction of the capillary pressure curves.

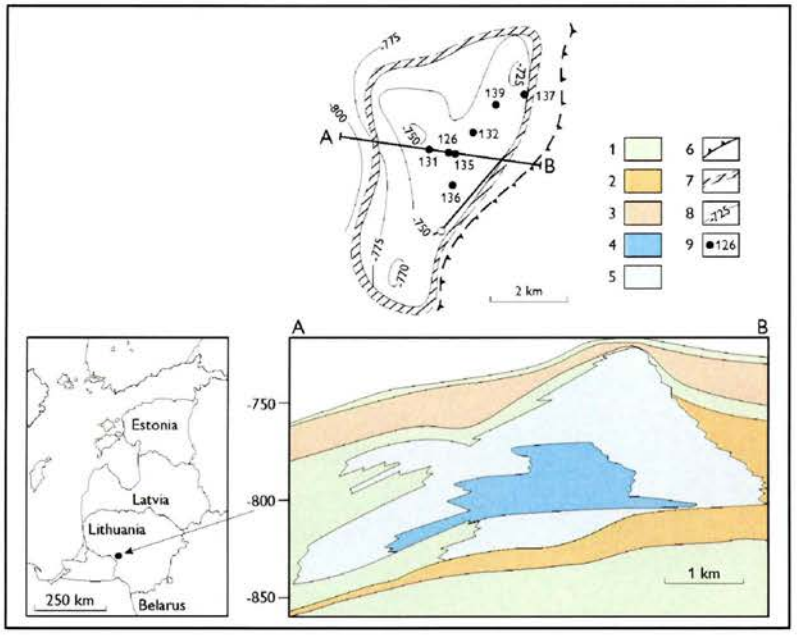
-775
-725
139
137
-800
-750
126
132
A
131
135
B
136
-750
-775
-770
2 km
1
2
3
4
5
6
7
8
9
126
A
B
Estonia
Latvia
Lithuania
250 km
Belarus
-750
-800
-850
1 km

Fig. 1

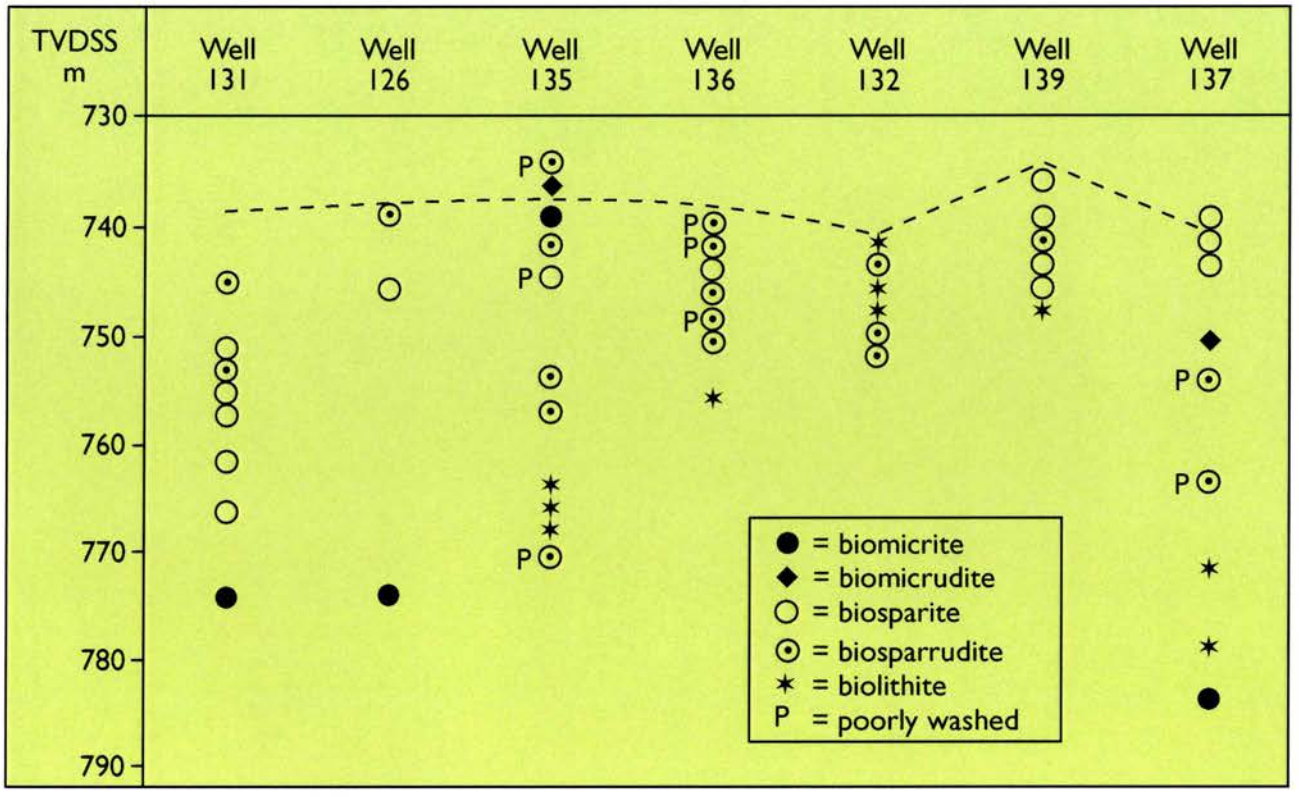
TVDSS
m
Well
131
Well
126
Well
135
Well
136
Well
132
Well
139
Well
137
730
740
750
760
770
780
790
P
= biomicrite
= biomicrudite
= biosparite
= biosparrudite
= biolithite
P = poorly washed

Fig. 2

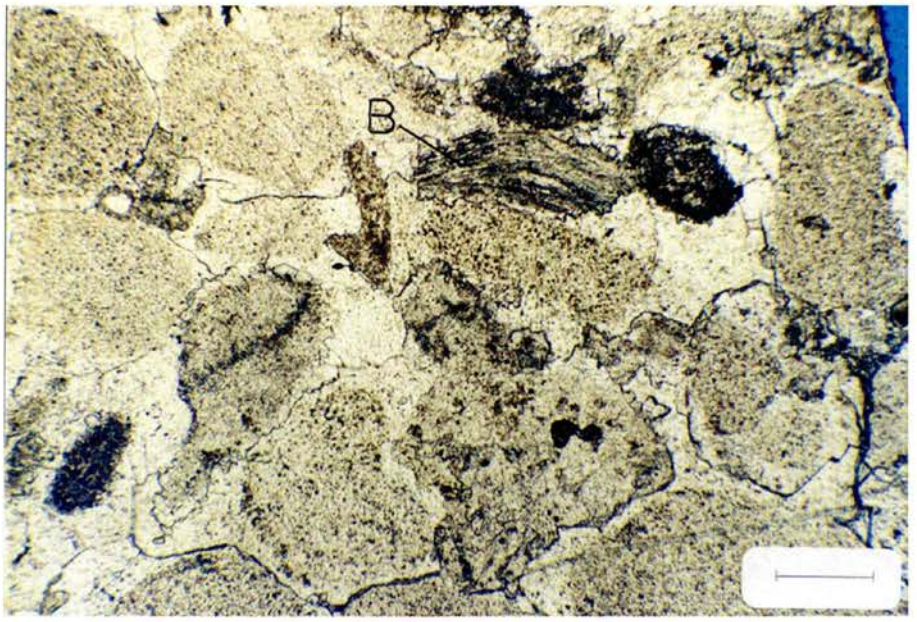

Fig. 3

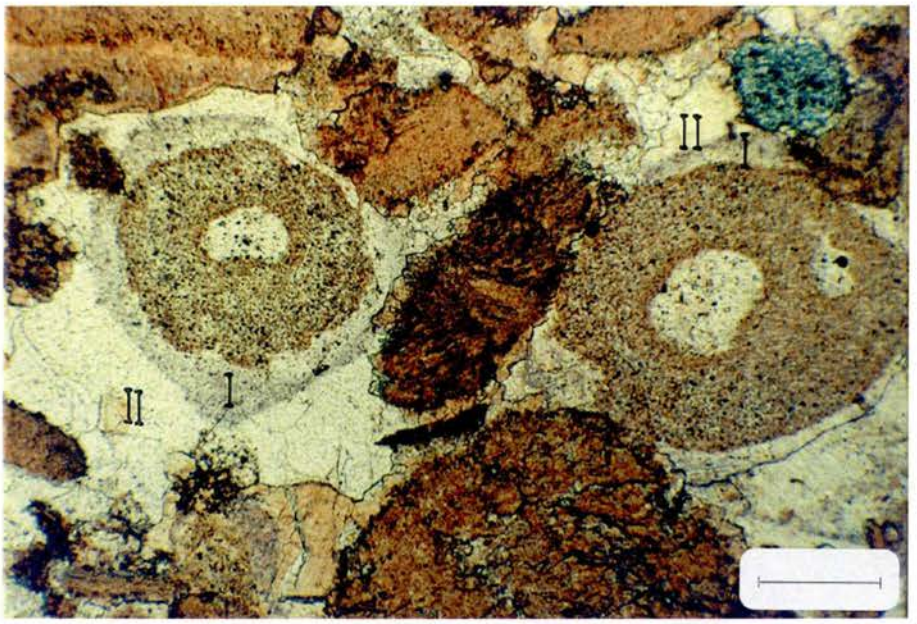

Fig. 4a

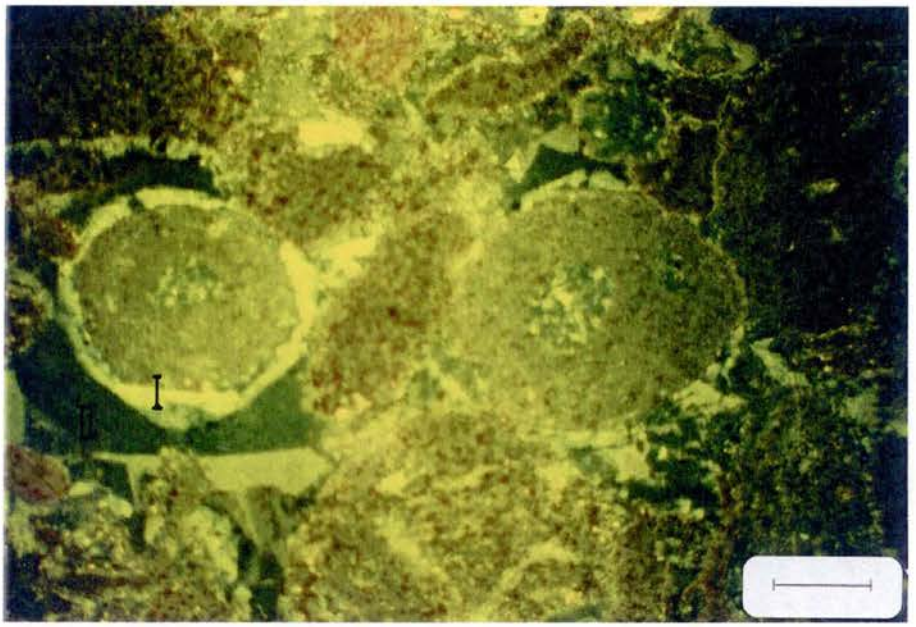

Fig. 4b

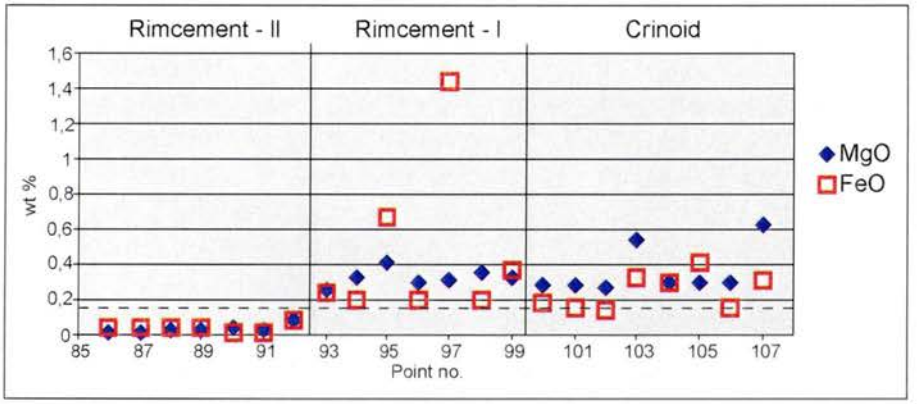
Rimcement - II
Rimcement - I
Crinoid
1,6
1,4
1,2
1
0,8
0,6
0,4
0,2
0
wt %
85
87
89
91
93
95
97
99
101
103
105
107
Point no.
MgO
FeO

Fig. 5

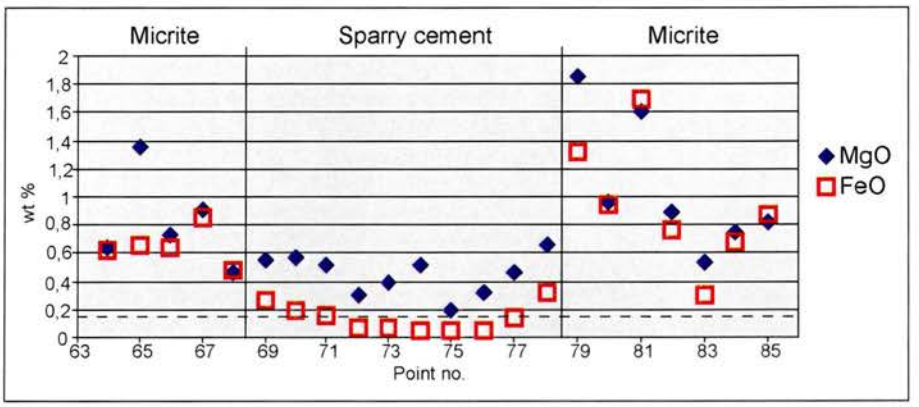
Micrite
Sparry cement
Micrite
wt %
2
1,8
1,6
1,4
1,2
1
0,8
0,6
0,4
0,2
0
63
65
67
69
71
73
75
77
79
81
83
85
Point no.
MgO
FeO

Fig. 6

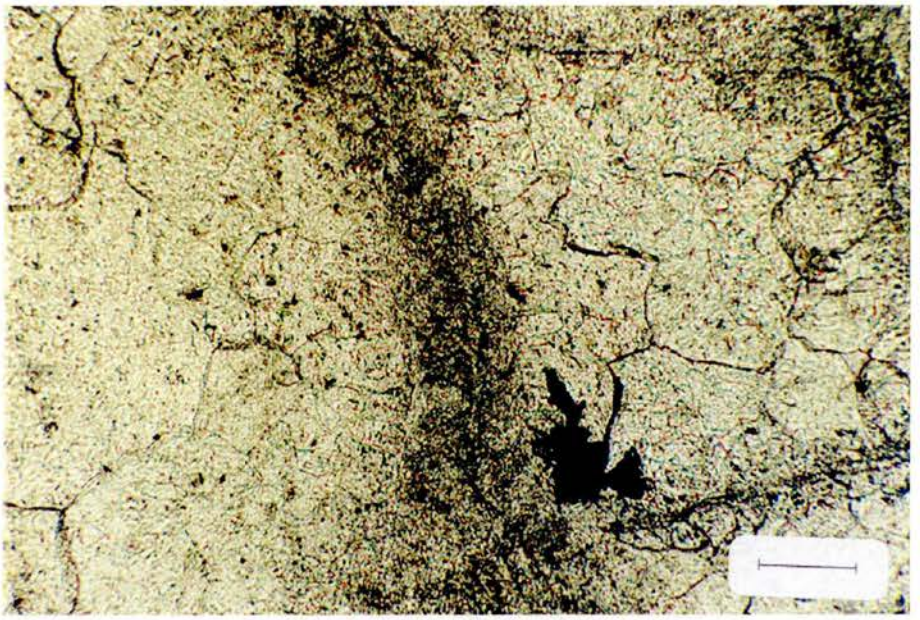

Fig. 7a

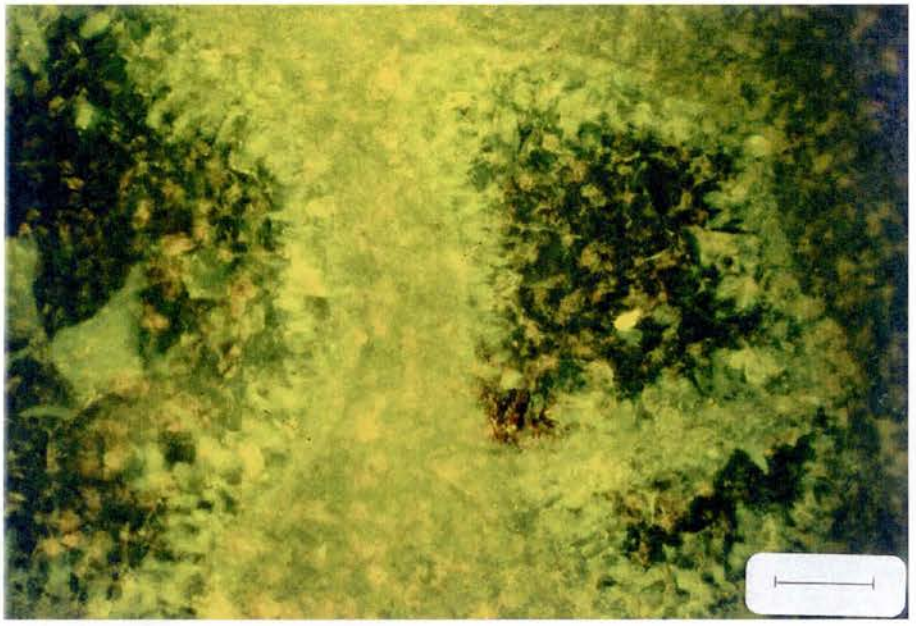

Fig. 7b

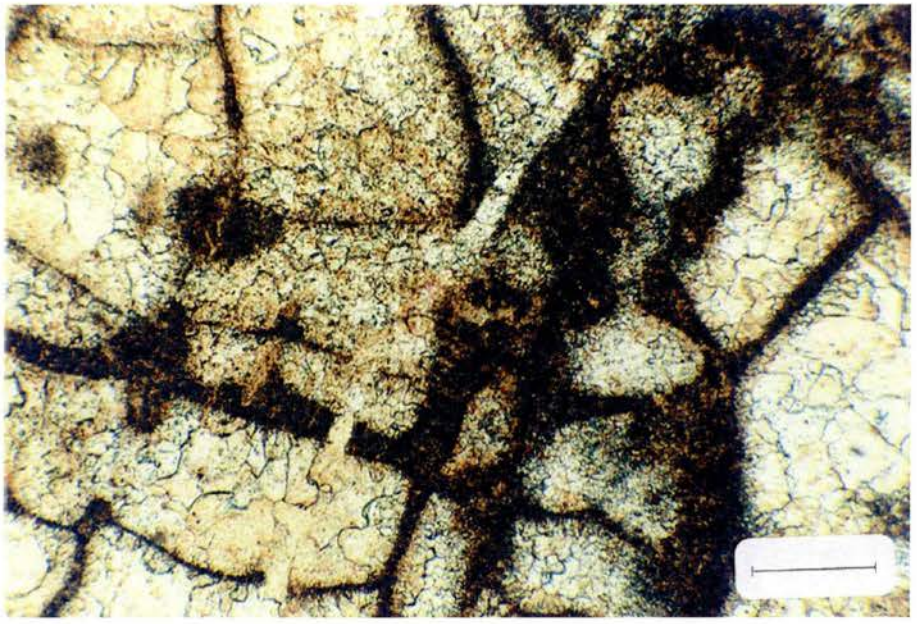

Fig. 8a

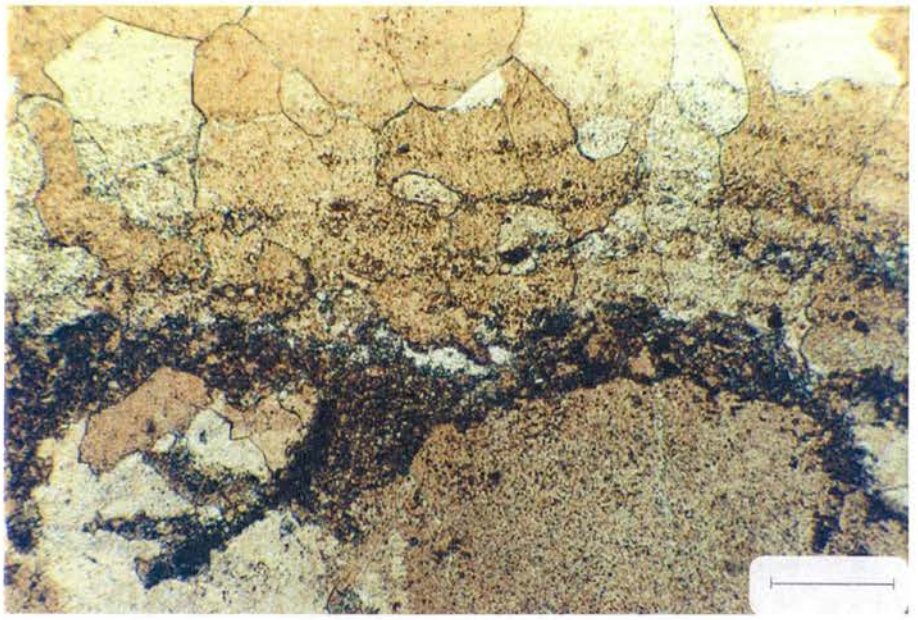

Fig. 8b

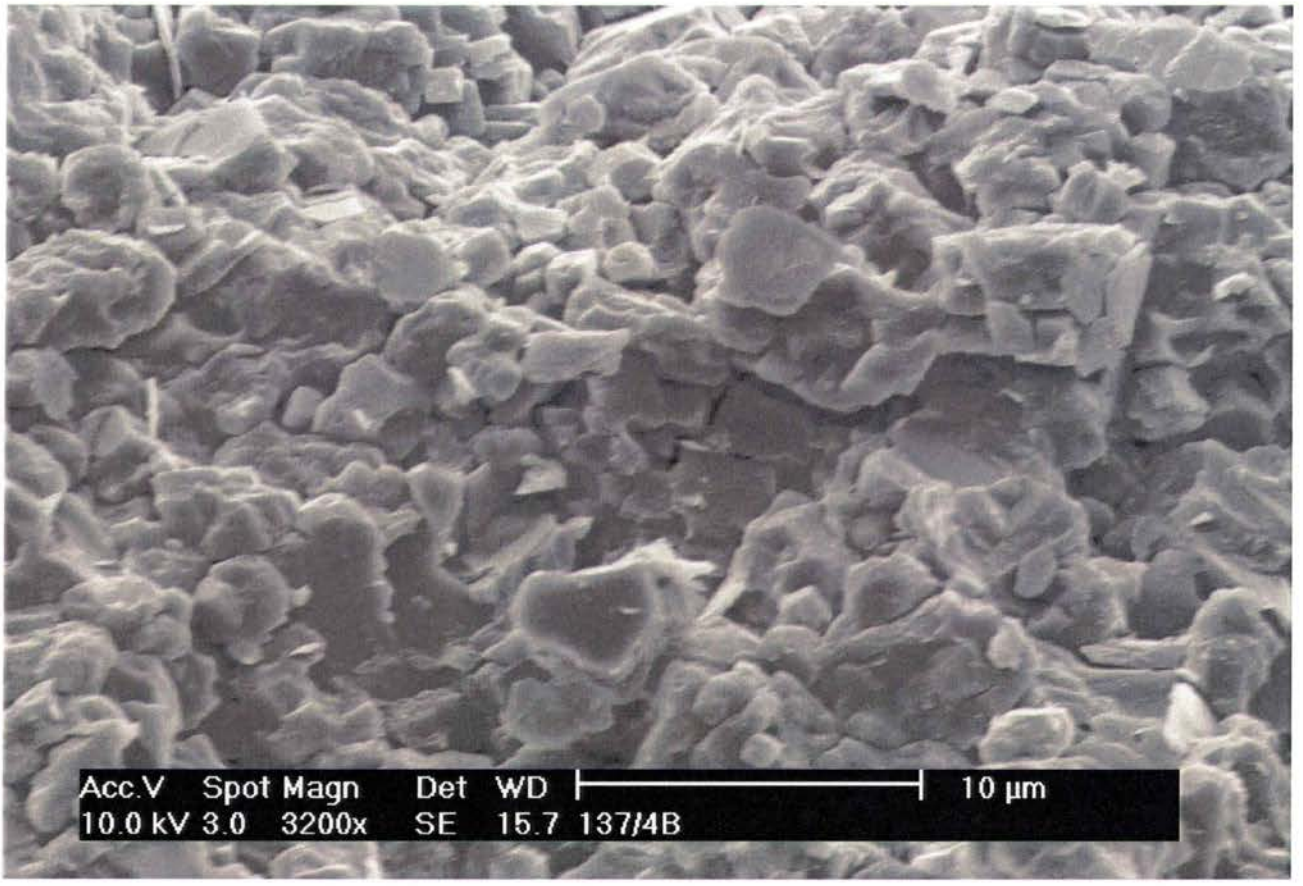

Fig. 9

Fig. 10

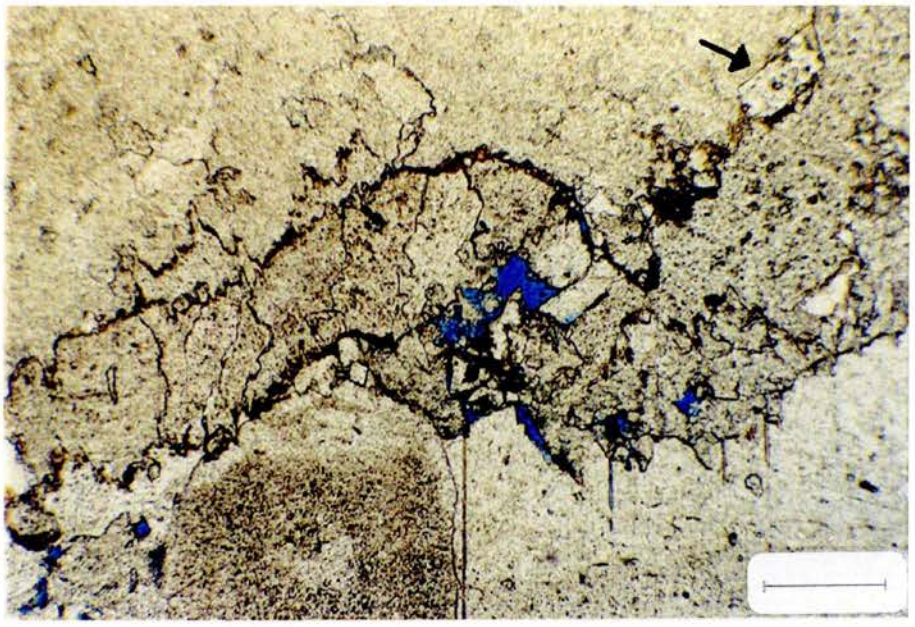

Fig. 11

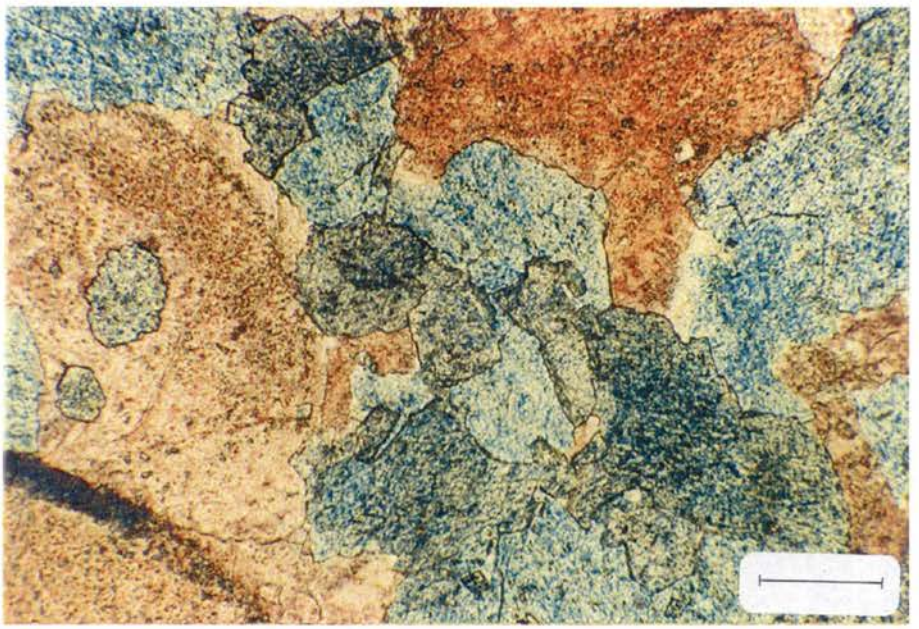

Fig. 12

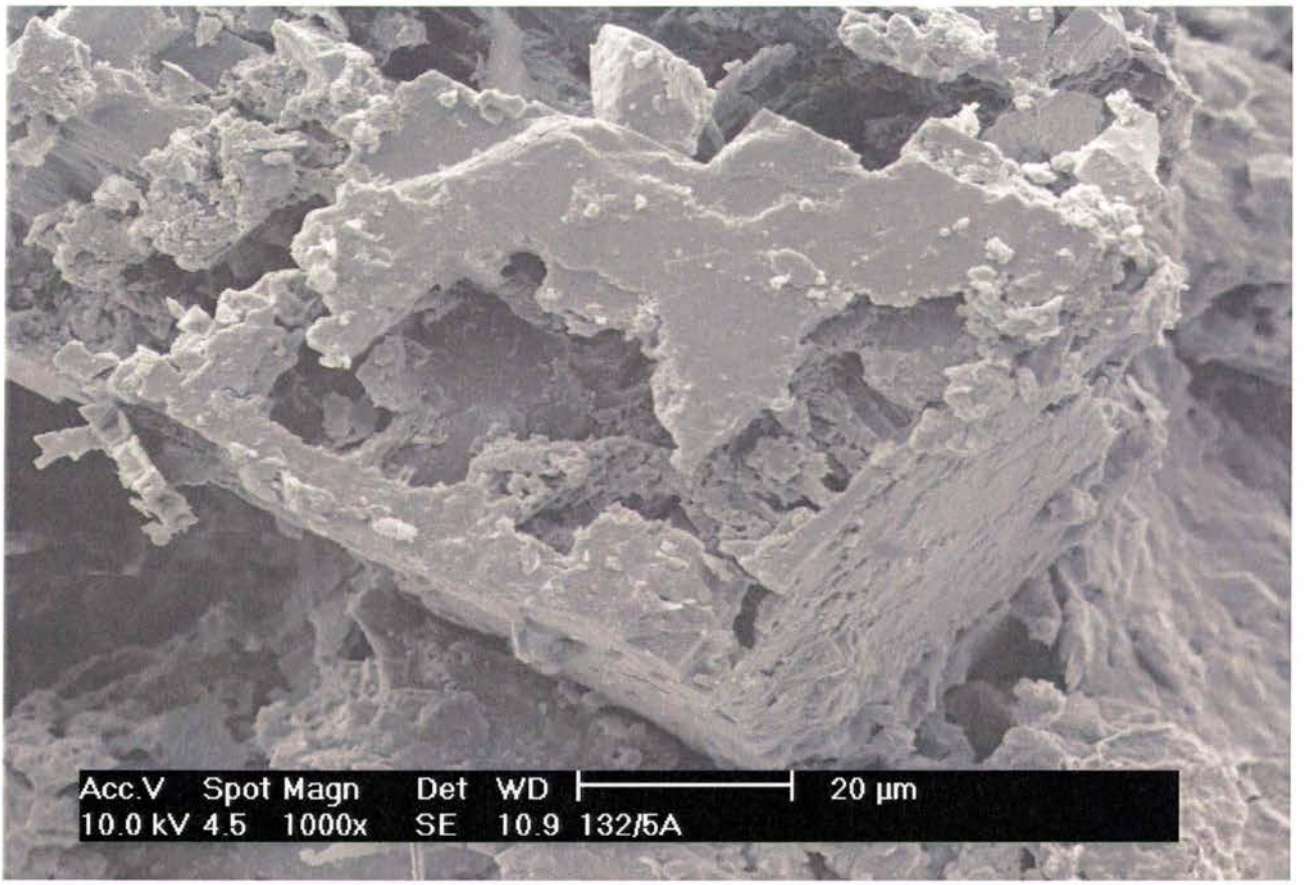

Fig. 13

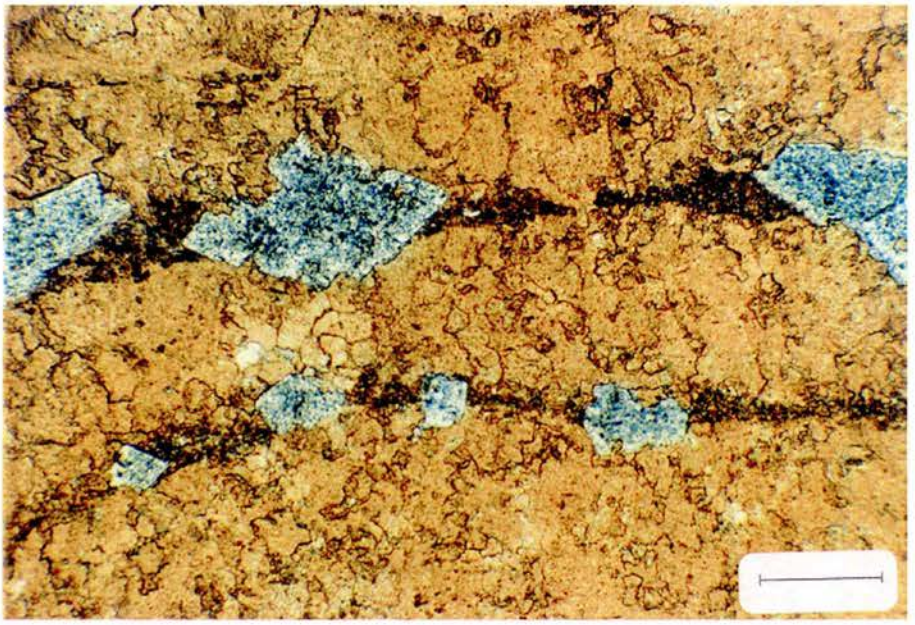

Fig. 14

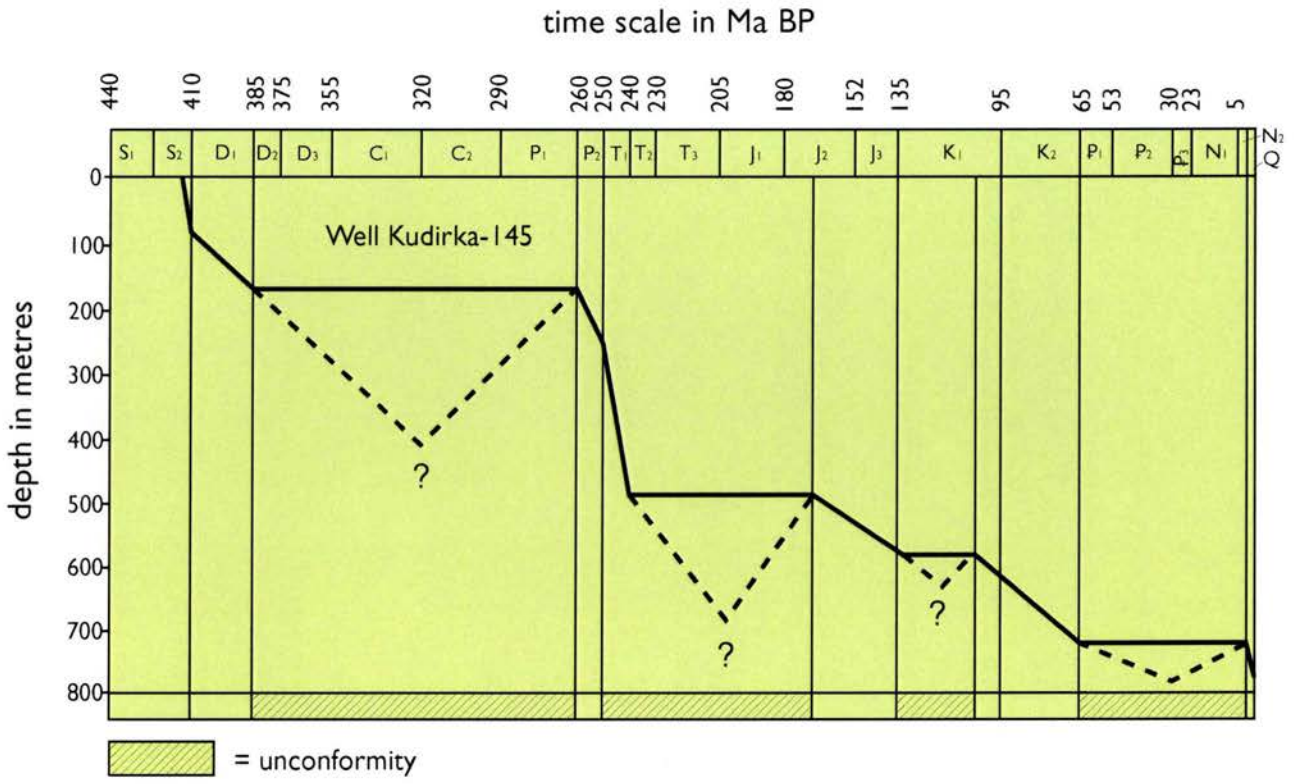
time scale in Ma BP
440
410
385
375
355
320
290
260
250
240
230
205
180
152
135
95
65
53
30
23
5
S1
S2
D1
D2
D3
C1
C2
P1
P2
T1
T2
T3
J1
J2
J3
K1
K2
P1
P2
P3
N1
Q
N2
0
100
200
300
400
500
600
700
800
depth in metres
Well Kudirka-145
?
?
?
?
= unconformity

Fig. 15

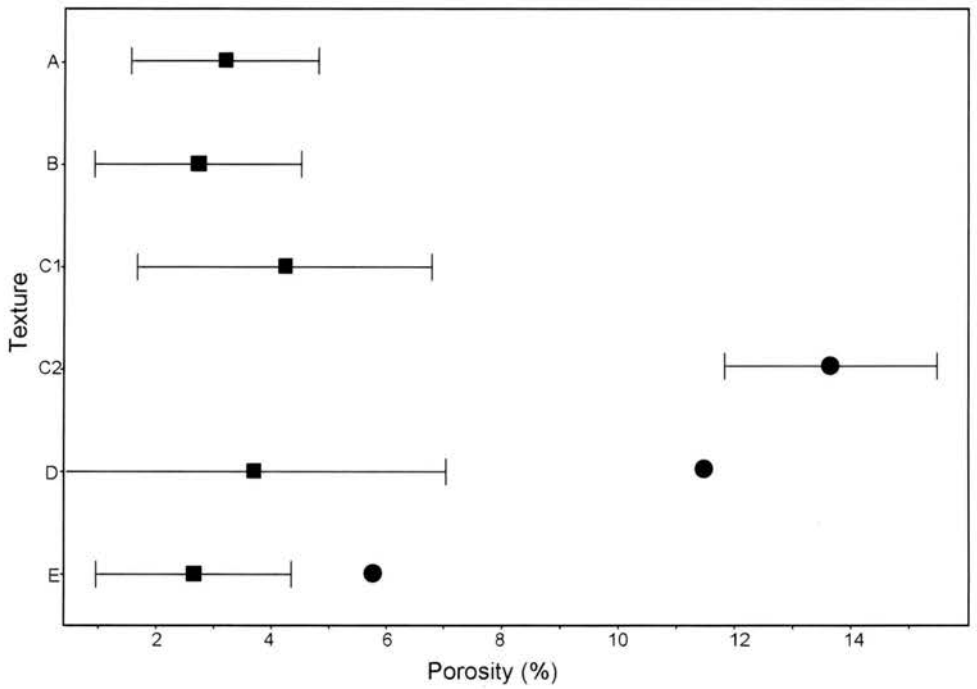
A
B
C1
C2
D
E
Texture
2
4
6
8
10
12
14
Porosity (%)

Fig. 16

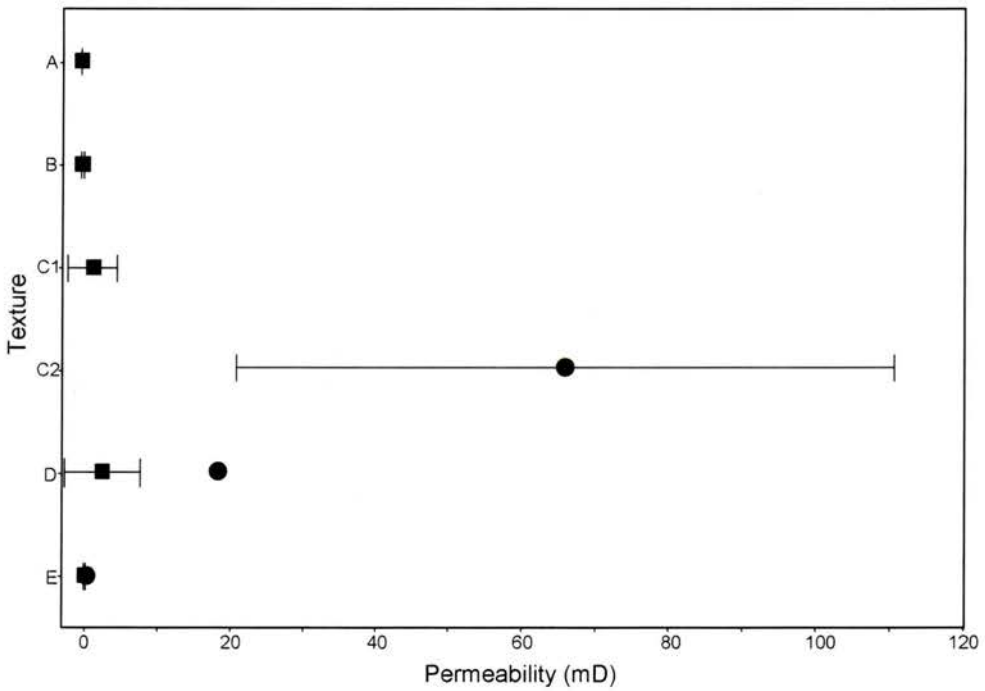
A
B
C1
C2
D
E
Texture
0
20
40
60
80
100
120
Permeability (mD)

Fig. 17

Rock texture (cf. Folk, 1962)	d = 0	0 < d < 2	d = 2 - 10	d > 10	Total of samples
Biomicrites/ biomicrudites	2	4			6
Biolithites	4	3	3		10
Poorly washed biosparites/ bioparrudites	1	5	1	1	8
Biosparrudites		6	5	1	12
Biosparites		7	5	2	14
Total of samples	7	25	14	4	$\Sigma = 50$

Table 1

Atomic %

Sample No.	Method of measurement	Ca	Mg	Fe	Ca/Mg	Ca/(Mg + Fe)
126/3B	Areal	27.8	19.8	1.6	1.4	1.3
	Spot	26.7	21.0	2.1	1.3	1.2
	Areal	27.5	20.2	2.0	1.4	1.2
	Spot	27.6	21.1	1.2	1.3	1.2
136/5B	Areal	27.1	20.7	1.3	1.3	1.2
	Areal	27.6	20.1	1.4	1.4	1.3
	Spot	26.7	21.6	1.5	1.2	1.2
Mean		27.3	20.6	1.6	1.3	1.2

Weight %

Sample No.	Method of measurement	Ca	Mg	Fe	Ca/Mg	Ca/(Mg + Fe)
126/3B	Areal	45.5	19.7	3.7	2.3	1.9
	Spot	43.6	20.8	4.8	2.1	1.7
	Areal	44.8	20.0	4.8	2.2	1.8
	Spot	45.4	21.0	2.7	2.1	1.9
136/5B	Areal	45.0	20.8	3.0	2.2	1.9
	Areal	45.4	20.0	3.2	2.3	2.0
	Spot	44.0	21.6	3.4	2.0	1.8
Mean		44.8	20.6	3.7	2.2	1.9

Table 2

Sample no.	Porosity (%)	Permeability (mD)	Swir (%) at 160 psi
126/2A	10.2	0.98	8.8
132/1B	10.0	14.1	14.0
136/4B	3.6	0.59	22.9
139/2A	14.6	110.0	10.6
139/7A	12.5	46.4	18.5

Table 3